Bifurcation in the rotational spectra of nonlinear symmetric triatomic molecules

I. N. Kozin and I. M. Pavlichenkov

Institute of Applied Physics, Russian Academy of Sciences, 603600 Nizhni Novgorod, Russia;
Kurchatov Institute Russian Scientific Center, 123182 Moscow, Russia
(Submitted 16 April 1997)
Zh. Éksp. Teor. Fiz. **112**, 1239–1256 (October 1997)

A microscopic theory is proposed for bifurcation in the rotational spectra of nonlinear AB_2-type molecules. The theory is based on a study of small-amplitude vibrational and precessional motion near the stationary states of a rotating molecule. Bifurcation leads to the formation of fourfold clusters of levels in the upper parts of the rotational multiplets, disruption of the symmetry of the molecule, and a transition from normal to local valence vibrations. The role of the centrifugal force of inertia in the development of these effects is clarified. Bifurcation and the accompanying phenomena are studied in the hydride molecules H_2O, H_2S, H_2Se, and H_2Te using empirical molecular potentials. © *1997 American Institute of Physics.* [S1063-7761(97)00710-5]

1. INTRODUCTION

The cluster structure of molecular rotational spectra is an interesting phenomenon which has attracted the interest of researchers for over two decades.[1–4] In the past, however, attention has mainly been devoted to highly symmetric molecules of the spherical top type. One of the authors of the present paper, together with Zhilinskii,[5] predicted the possible formation of fourfold cluster states in the upper parts of the rotational multiplets of symmetric nonlinear triatomic molecules with the structure of an asymmetric top. The classical vibrational–rotational dynamics of these molecules has been studied using a model[6] of rigid valence bonds. It was shown that as the total angular momentum J of the molecule[1)] increases, local precession about the axis with the lowest moment of inertia evolves into delocalized precession about two equivalent axes lying in the plane of the molecule. The change in the rotational dynamics is caused by bifurcation at a critical point $J=J_c$. Bifurcation shows up as a softening of the precessional mode, i.e., the upper levels of the rotational multiplets come closer with increasing J. Prior to the prediction of this effect, experimental data showed a distinct convergence of levels in vibrational bands (ground state and ν_2) of the H_2O and H_2S molecules.[5,7] The observed effect was so unusual from the standpoint of existing concepts of rotation in asymmetric-top molecules, that immediately after the appearance of Ref. 5 numerical calculations of the rotational spectrum of water using a model of rigid valence bonds were published[8] which confirmed the level convergence effect.

The simplest theory of bifurcation proposed in Ref. 5 made it possible to estimate the critical angular momentum J_c.[9,7] It turned out that J_c decreases as the mass of the central core of the molecule increases. This result has been used in experimental studies of level clustering in the ground vibrational state of the H_2Se molecule.[10,11] It was found that, indeed, groups of four quasidegenerate levels (clusters) begin to form in the upper parts of the J-multiplets of this molecule for $J>J_c$. An analogous effect has recently been observed experimentally in H_2Te.[12] The MORBID method, which is based on numerical solutions of the Schrödinger equation, has been used successfully to describe cluster states in H_2Se,[13,14] H_2S,[15] and H_2Te.[16] The variational program MORBID[17] can be used to find the energy levels of the complete vibrational–rotational Hamiltonian of a molecule in an isolated electronic state. Calculations using realistic potentials, both *ab initio* and fitted to experimental data, reproduce well the observed energy levels of the rotational multiplets and can be used to follow the evolution of clusters in the ground vibrational state of the H_2Se, H_2S, and H_2Te molecules as J increases. These calculations agree with classical, semiclassical, and model quantum mechanical estimates of the magnitude of J_c. At the same time, numerical calculations of the rotational levels of the ground state band of the water molecule up to $J\sim 40$ using[18] the potential of Jensen *et al.*[19] and subsequently[20] with a more exact empirical potential have not revealed any distinct fourfold clusters. These results contradict estimates of the classical angular momentum for the H_2O molecule given in Refs. 5 ($J_c=27-28$) and 8 ($J_c=26$).

In this paper we eliminate the deficiency inherent in the model of absolutely rigid bonds. Bifurcation in the rotational spectrum of symmetric triatomic molecules is analyzed on the basis of the exact vibrational–rotational Hamiltonian obtained in Sec. 2. Classical equations are used for the vibrational–rotational motion of the molecules, since we are considering phenomena at large J and the de Broglie wavelengths of the nuclei are much shorter than the molecular dimensions. In Sec. 3 the stationary states of the system are found and in Secs. 4 and 5 the variations in the vibrational–rotational dynamics of the system are studied as functions of its total angular momentum. A method based on an examination of small harmonic oscillations (classical and quantum mechanical) near the stationary states of a rapidly rotating molecule is used.[21] The four-mode motion can be separated into a slow precession near the stationary rotation axis and fast vibrations near an equilibrium configuration that does not coincide with the configuration of the molecule in its ground state. This approach differs from the widely used Wilson–Decius–Cross theory[22] in that the vibrational and rotational degrees of freedom are separated near the station-

ary state of the rapidly rotating molecule. Because of centrifugal forces, this difference leads to some new phenomena: the precession of an AB_2 molecule about the axis with a minimum moment of inertia becomes unstable at the bifurcation point J_c. At high J, the molecule rotates uniformly about one of two equivalent (owing to the C_{2v} symmetry) axes located in the plane of the molecule between the principal axes with the minimum and intermediate moments of inertia. Quantum delocalization of the precession can lead to fourfold clusters in the rotational multiplets which are the spectroscopic manifestation of bifurcation. Another consequence is an asymmetric deformation of the molecule by the centrifugal forces of inertia. As a result, one of the A−B bonds becomes longer than the other, which in turn changes the vibrational dynamics of the molecule: the normal valence vibrations ν_1 and ν_3 change into local vibrations of the two A−B bonds. The transition discussed in Section 5 is in no way related to the anharmonicity of the vibrations, as happens in the generally accepted theory,[23] but is a consequence of the disruption of the symmetry of the molecule by the bifurcation. As applications of the theory we consider the hydrides H_2O, H_2S, H_2Se, and H_2Te, whose vibrational–rotational motion is still adiabatic compared to the electronic motion (despite the high J) and have energies lower than the dissociation energy of the molecules. In this series, the water molecule occupies a special place, demonstrating that level clustering is not, in general, a necessary consequence of bifurcation.

2. THE CLASSICAL VIBRATIONAL–ROTATIONAL HAMILTONIAN

Our derivation of the classical vibrational–rotational Hamiltonian is, on the whole, close to that of Wilson, Decius, and Cross.[22] The difference is that we do not use normal coordinates, since we are considering configurations which differ greatly from that of the molecular ground state. The kinetic energy of a molecule in the rotating coordinate system has the form

$$T=\frac{1}{2}\sum_{ij}\omega_i I_{ij}\omega_j+\sum_i \omega_i L_i+\frac{1}{2}\sum_{\lambda i} m_\lambda v_{\lambda i}^2, \tag{1}$$

where the subscripts i and j denote the x, y, and z axes of this system, ω_i are the projections of the angular velocity, and I_{ij} is the moment of inertia tensor of the molecule. The position of the nucleus λ with mass m_λ is given by the vector $\mathbf{r}_\lambda$ $(x_\lambda, y_\lambda, z_\lambda)$, its velocity is $\mathbf{v}_\lambda$, and $\mathbf{L}=\Sigma_\lambda m_\lambda \mathbf{r}_\lambda \times \mathbf{v}_\lambda$ is the angular momentum of the vibrational motion of the nuclei.

Let us consider a triatomic molecule $B_1A_2B_3$ with nuclear masses $m_1=m_3=m$ and $m_2=M$ and define a rotating coordinate system as follows:[24] place the molecule in the xz plane (i.e., $y_\lambda=0$) so that the bisector of the valence angle $\alpha=\widehat{B_1A_2B_3}$ is parallel to the x axis. The z axis is directed from nucleus B_3 to nucleus B_1, while the x axis is directed from the center of mass to nucleus A_2. In the following we also introduce the internal coordinates $q_1=r_1$ (the A_2-B_1 distance), $q_2=\alpha$ and $q_3=r_3$ (the A_2-B_3 distance). The internal coordinates are related to the projections of the vector $\mathbf{r}$ as follows:

$$\begin{aligned}
x_1&=-\frac{(M+m)r_1-mr_3}{M+2m}\cos\frac{\alpha}{2},\\
x_2&=\frac{m(r_1+r_3)}{M+2m}\cos\frac{\alpha}{2},\\
x_3&=\frac{mr_1-(M+m)r_3}{M+2m}\cos\frac{\alpha}{2},\\
z_1&=\frac{(M+m)r_1+mr_3}{M+2m}\sin\frac{\alpha}{2},\\
z_2&=-\frac{m(r_1-r_3)}{M+2m}\sin\frac{\alpha}{2},\\
z_3&=-\frac{mr_1+(M+m)r_3}{M+2m}\sin\frac{\alpha}{2}.
\end{aligned} \tag{2}$$

With this choice of a rotating coordinate system, the nonzero components of the inertia tensor are

$$\begin{aligned}
I_{xz}&=\frac{m(M+m)}{2(M+2m)}(r_1^2-r_3^2)\sin\alpha,\\
I_{xx}&=\frac{m}{M+2m}[M(r_1^2+r_3^2)+m(r_1+r_3)^2]\sin^2\frac{\alpha}{2},\\
I_{zz}&=\frac{m}{M+2m}[M(r_1^2+r_3^2)+m(r_1-r_3)^2]\cos^2\frac{\alpha}{2},\\
I_{yy}&=\frac{m(M+m)}{M+2m}(r_1^2+r_3^2)-\frac{2m^2}{M+2m}r_1r_3\cos\alpha.
\end{aligned} \tag{3}$$

We write the components of the vector $\mathbf{L}$ in the form $L_i=\Sigma_\nu G_{i\nu}\dot{q}_\nu$, where only three elements of the mixed matrix $\mathbf{G}$ are nonzero (the subscript ν refers to the internal coordinates):

$$\begin{aligned}
G_{y1}&=-\frac{m^2}{M+2m}r_3\sin\alpha,\\
G_{y2}&=\frac{m(M+m)}{2(M+2m)}(r_1^2-r_3^2),\\
G_{y3}&=\frac{m^2}{M+2m}r_1\sin\alpha.
\end{aligned} \tag{4}$$

The kinetic energy (1) in the new coordinates is

$$T=\frac{1}{2}\sum_{ij}\omega_i I_{ij}\omega_j+\sum_{i\nu}\omega_i G_{i\nu}\dot{q}_\nu+\frac{1}{2}\sum_{\nu\nu'}\dot{q}_\nu a_{\nu\nu'}\dot{q}_{\nu'}, \tag{5}$$

where the matrix $\mathbf{a}$ has the elements

$$\begin{aligned}
a_{11}&=a_{33}=\frac{m(M+m)}{M+2m},\\
a_{12}&=a_{21}=\frac{m^2}{2(M+2m)}r_3\sin\alpha,\\
a_{22}&=\frac{m}{4(M+2m)}[(M+m)(r_1^2+r_3^2)+2mr_1r_3\cos\alpha],
\end{aligned}$$

$$a_{23}=a_{32}=\frac{m^2}{2(M+2m)}\,r_1\,\sin\,\alpha,$$

$$a_{13}=a_{31}=-\frac{m^2}{M+2m}\cos\,\alpha. \tag{6}$$

In order to obtain the equations of motion in Hamiltonian form, we introduce the total angular momentum **J** of the molecule, which is related to its angular velocity by the equation[22]

$$J_i=\sum_j\,I_{ij}\omega_j+L_i, \tag{7}$$

and the momenta

$$p_\nu=\frac{\partial T}{\partial\dot q_\nu}=\sum_\nu\,a_{\nu\nu'}\dot q_{\nu'}+\omega_y G_{y\nu}, \tag{8}$$

conjugate to the internal coordinates q_ν. It follows from the last equation that the Coriolis force in the rotating molecule (given by the second term in Eq. (5)) is analogous to a magnetic field, since $\mathbf{p}\neq 0$ holds when $\dot{\mathbf{q}}=0$. Solving Eq. (7) for ω_j, we find

$$\omega_j=\sum_i\,\mathring{\mu}_{ji}(J_i-L_i). \tag{9}$$

where $\mathring{\boldsymbol{\mu}}$ is the inverse matrix of **I** with elements

$$\begin{aligned}&\mathring{\mu}_{xy}=\mathring{\mu}_{yz}=0,\quad \mathring{\mu}_{yy}=1/I_{yy},\\ &\mathring{\mu}_{xx}=I_{zz}/(I_{zz}I_{xx}-I_{xz}^2),\\ &\mathring{\mu}_{xz}=-I_{xz}/(I_{zz}I_{xx}-I_{xz}^2),\quad \mathring{\mu}_{zz}=I_{xx}/(I_{zz}I_{xx}-I_{xz}^2).\end{aligned} \tag{10}$$

Expressing $\dot{\mathbf{q}}$ in terms of **p** and **J** with the aid of Eqs. (8) and (9), we find the Hamiltonian of the rotating AB_2 molecule after some simple transformations:

$$H=\frac{1}{2}\sum_{ij}\,J_i\mu_{ij}J_j-J_y\sum_\nu\,u_{y\nu}p_\nu+\frac{1}{2}\sum_{\nu\nu'}\,p_\nu b_{\nu\nu'}p_{\nu'}+V(r_1,\alpha,r_3), \tag{11}$$

where $u_{y\nu}=\mathring{\mu}_{yy}\Sigma_{\nu'}G_{y\nu'}b_{\nu'\nu}$ and $\boldsymbol{\mu}$ is the matrix $\mathring{\boldsymbol{\mu}}$ modified by the Coriolis force. In our case, all the elements μ_{ij} are equal to $\mathring{\mu}_{ij}$ (10) except $\mu_{yy}=\mathring{\mu}_{yy}(1+\Sigma_\nu G_{y\nu}u_{y\nu})$. The matrix **b** is defined by the equation

$$\mathbf{b}=(\mathbf{a}-\mathbf{G}^T\mathring{\boldsymbol{\mu}}\mathbf{G})^{-1}. \tag{12}$$

where $\mathbf{G}^T$ is the transposed matrix. The elements of the matrix **b** are given by[22]

$$\begin{aligned}&b_{11}=b_{33}=\frac{1}{M}+\frac{1}{m},\quad b_{12}=b_{21}=-\frac{\sin\,\alpha}{Mr_3},\\ &b_{22}=\left(\frac{1}{M}+\frac{1}{m}\right)\left(\frac{1}{r_1^2}+\frac{1}{r_3^2}\right)-\frac{2\cos\,\alpha}{Mr_1r_3},\\ &b_{23}=b_{32}=-\frac{\sin\,\alpha}{Mr_1},\quad b_{13}=b_{31}=\frac{\cos\,\alpha}{M}.\end{aligned} \tag{13}$$

Finally, the last term in Eq. (11) is the potential V of the interaction of the nuclei in the molecule, which is a symmetric function with respect to interchange of identical nuclei.

The equations of motion for the Hamiltonian (11) have the form

$$\dot q_\nu=\sum_{\nu'}\,b_{\nu\nu'}p_{\nu'}-J_y u_{y\nu}, \tag{14}$$

$$\dot p_\nu=-\frac{1}{2}\sum_{ij}\,J_i\frac{\partial\mu_{ij}}{\partial q_\nu}J_j+J_y\sum_{\nu'}\,\frac{\partial u_{y\nu'}}{\partial q_\nu}p_{\nu'}-\frac{1}{2}\sum_{\nu'\nu''}\,p_{\nu'}\frac{\partial b_{\nu'\nu''}}{\partial q_\nu}p_{\nu''}-\frac{\partial V}{\partial q_\nu}. \tag{15}$$

and

$$\dot J_i=\sum_{jkl}\,e_{ijk}J_j\mu_{kl}J_l+\sum_{k\nu}\,e_{iyk}u_{y\nu}J_k p_\nu. \tag{16}$$

The last equation is obtained using the Poisson brackets $\{J_i,J_j\}=e_{ijk}J_k$, where e_{ijk} is the asymmetric unit tensor. It is easy to see that $\mathbf{J}^2$ is a constant of motion for Eqs. (14)–(16). In addition, the Hamiltonian and the equations of motion are invariant with respect to the $C_{2v}(M)$ group of the AB_2 molecule.[25,26]

3. STATIONARY STATES OF A ROTATING MOLECULE

First we shall find the stationary points of the equations of motion. Equating the time derivatives in Eqs. (14)–(16) to zero, we obtain a system of nonlinear algebraic equations which determine the configuration of the molecule and its axis of uniform rotation. In particular, Eq. (16) and the condition that $\mathbf{J}^2$ be conserved yield the stationary angular momentum $\mathbf{J}_s$ in the proper coordinate system. The three projections of this vector can satisfy the four equations if at least one of them is equal to zero. Thus, there are two types of stationary states, axial and planar. For small J only the axial states S_i exist: $J_{si}=\pm J$, $i=x, y, z$, in which the molecule rotates about one of the principal axes of inertia. Because the molecule is flat, the Coriolis force shows up only in the S_y state, which leads to a nonzero momentum with components

$$p_{\nu s}=J\sum_{\nu'}\,c_{\nu\nu'}u_{y\nu'}. \tag{17}$$

As a result, the additional term in the expression for μ_{yy} vanishes and the rotation of the molecule about the y axis is characterized by the moment of inertia I_{yy}. The equilibrium configuration of the molecule in state S_i is determined by the equations

$$\frac{1}{2}\frac{\partial\mathring{\mu}_{ii}}{\partial q_\nu}J^2+\frac{\partial V}{\partial q_\nu}=0,\quad \nu=1, 2, 3, \tag{18}$$

which are found from Eqs. (14) and (15). In the axial stationary state, the molecule has a symmetric configuration with bond lengths $r_{1s}=r_{3s}=r_s$, a valence angle α_s, and energies

$$E_i=\frac{J^2}{2I_{ii}(r_s,\alpha_s,r_s)}+V(r_s,\alpha_s,r_s). \tag{19}$$

TABLE I. The change $\Delta r_\nu = r_{\nu s} - r_{\nu e}$ in bond lengths owing to the centrifugal force in the S_{xz} stationary state for $J=20$ (it is assumed that the molecule rotates about an axis approximately perpendicular to the r_1 bond).

	Quantum mechanical calculation		Classical calculation	
Molecule	Δr_1, Å	Δr_3, Å	Δr_1, Å	Δr_3, Å
H_2Se	0.023 [14]	0.004 [14]	0.025	0.002
H_2S	0.024 [15]	0.009 [15]	0.022	0.010

This state is doubly degenerate in the direction of the total angular momentum. In the following we shall distinguish the equilibrium configurations of rotating and nonrotating molecules by the subscripts s and e.

We now consider the plane stationary state S_{xz} in which the molecule rotates around one of two equivalent axes, z' or z'', located in the xz plane symmetrically with respect to the x axis and forming angles β_s and $\pi-\beta_s$, respectively, with the z axis. The configuration of the molecule and the angle β_s are determined by the equations

$$\frac{1}{2}\left(\frac{\partial \mathring{\mu}_{xx}}{\partial q_\nu}\sin^2\beta_s+\frac{\partial \mathring{\mu}_{xz}}{\partial q_\nu}\sin 2\beta_s+\frac{\partial \mathring{\mu}_{zz}}{\partial q_\nu}\cos^2\beta_s\right)J^2+\frac{\partial V}{\partial q_\nu}=0,\quad \nu=1,2,3. \tag{20}$$

and

$$\frac{1}{2}(\mathring{\mu}_{xx}-\mathring{\mu}_{zz})\sin 2\beta_s+\mathring{\mu}_{xz}\cos 2\beta_s=0. \tag{21}$$

In the S_{xz} state the molecule has an asymmetric configuration with unequal bond lengths r_{1s} and r_{3s}. Of the two bonds, the one which forms the larger angle with the rotation axis is the longer (for example, r_{1s} for the z' axis). As J increases it is stretched by the centrifugal force and tends to be perpendicular to the axis of rotation. The symmetry disruption effect is illustrated in Table I, which lists the amounts of change in the bond lengths in the S_{xz} state relative to the equilibrium value for the nonrotating molecule. These results were obtained by classical and quantum mechanical calculations using empirical potentials for the H_2Se (Ref. 13) and H_2S (Ref. 15) molecules. The two methods appear to give approximately the same results.

Let us turn the coordinate system through an angle β around the y axis. Using Eq. (10) and noting that $I_{xx}I_{zz}-I_{xz}^2$ is invariant with respect to rotations, we find the relation between the matrix elements of the inverse moment of inertia in the initial (xyz) and rotated $(x'yz')$ systems to be

$$\begin{aligned}
\mathring{\mu}_{x'x'}&=\mathring{\mu}_{xx}\cos^2\beta+\mathring{\mu}_{zz}\sin^2\beta-\mathring{\mu}_{xz}\sin 2\beta,\\
\mathring{\mu}_{x'z'}&=-\frac{1}{2}(\mathring{\mu}_{xx}-\mathring{\mu}_{zz})\sin 2\beta-\mathring{\mu}_{xz}\cos 2\beta,\\
\mathring{\mu}_{z'z'}&=\mathring{\mu}_{xx}\sin^2\beta+\mathring{\mu}_{zz}\cos^2\beta+\mathring{\mu}_{xz}\sin 2\beta.
\end{aligned} \tag{22}$$

Comparing the expression for $\mathring{\mu}_{x'z'}$ with Eq. (21), we find that the z' axis (as well as the z'' axis) is the principal axis of inertia of an asymmetric molecule with a moment of inertia of

$$I_{z'z'}=\frac{1}{2}\left[I_{xx}+I_{zz}+\sqrt{(I_{xx}-I_{zz})^2+4I_{xz}^2}\right]. \tag{23}$$

Thus, the plane state S_{xz} with energy

$$E_{xz}=\frac{J^2}{2I_{z'z'}}+V(r_{1s},\alpha_s,r_{3s}) \tag{24}$$

is fourfold degenerate. It has a lower symmetry than the axial state. This means that a transition from the axial sate S_z into the plane state with increasing J is accompanied by a C_{2v} type bifurcation.[7] Up to the bifurcation point J_c, a symmetric molecule rotates around the axis with the minimum moment of inertia I_{zz}. In the region $J>J_c$, an asymmetric molecule rotates around the principal axis with an intermediate moment of inertia $I_{z'z'}$. This ensures that the energy of a uniformly rotating molecule and its first derivative with respect to J are continuous at the critical point J_c. A change in the rotation regimes leads to an increase in the rotation energy in the S_{xz} state compared to the state S_z, i.e., to an increase in the energy of the upper level of the multiplet.

The equilibrium configuration of a uniformly rotating molecule is found according to Eqs. (18) and (19) from requiring the time-independence of the effective potential

$$V_{\text{eff}}=\frac{1}{2}\sum_{ij}J_i\mathring{\mu}_{ij}J_j+V. \tag{25}$$

On the other hand, the effective potential in the equilibrium configuration is equal to the energy of the corresponding stationary state, as this follows from Eqs. (19) and (24). The competition between the centrifugal and potential terms of Eq. (25) determines the change in the molecular configuration as J increases. Let us first examine the state S_z. Differentiating Eq. (18) with respect to J yields the following formulas:

$$\begin{aligned}
\frac{dr_1}{dJ}&=\frac{dr_3}{dJ}=\frac{J}{r_s I_{zz}}\left(\frac{\partial^2 V_{\text{eff}}}{\partial r_1^2}\right)_s^{-1},\\
\frac{d\alpha}{dJ}&=-\frac{J}{I_{zz}}\left(\frac{\partial^2 V_{\text{eff}}}{\partial \alpha^2}\right)_s^{-1}\tan\frac{\alpha_s}{2},
\end{aligned} \tag{26}$$

valid in the approximation

$$\left(\frac{\partial^2 V_{\text{eff}}}{\partial q_\nu^2}\right)_s \gg \left|\frac{\partial^2 V_{\text{eff}}}{\partial q_\nu \partial q_{\nu'}}\right|_s,\quad \nu\neq\nu', \tag{27}$$

which is satisfied for all the hydrides under consideration. Thus, in the stationary state S_z the bond lengths increase, while the valence angle decreases, with increasing J.

The approximation (27) is not applicable in the S_{xz} state and the change in the equilibrium configuration of the molecule as J increases depends on the features of its molecular potential. The rate of change of the coordinates of the equilibrium configuration is determined by the equation

$$\frac{dq_\nu}{dJ}=-\sum_{\nu'}g^{-1}_{\nu\nu'}\left(\frac{\partial \mathring{\mu}_{z'z'}}{\partial q_{\nu'}}\right)_s, \tag{28}$$

where $\mathbf{g}$ is the matrix of the second derivatives of V_{eff} at the stationary point. For rotation about the z' axis the bond length r_{1s} increases, while r_{3s} initially decreases and then

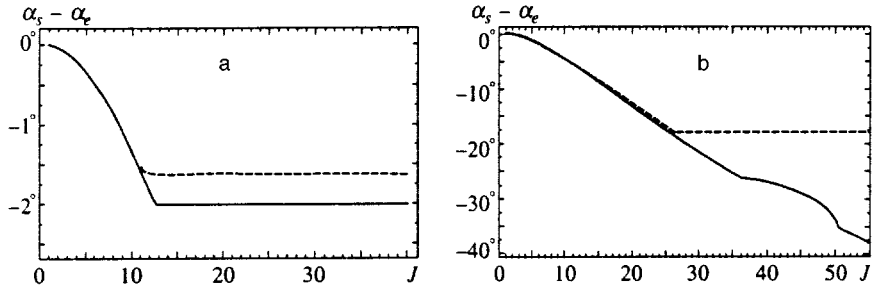

FIG. 1. The dependence on angular momentum J of the relative change in the valence angle in the stationary states S_z ($J<J_c$) and S_{xz} ($J>J_c$) corresponding to the upper level of the rotational multiplets of the ground state of the H_2Se (a) and H_2O (b) molecules. The smooth curves are calculations according to Eqs. (18), (20), and (21) ($J_c=13$ for H_2Se and 36 for H_2O); the dashed curves are from the absolutely rigid bond model ($J_c=12$ for H_2Se and 27 for H_2O).

slowly increases with rising J. For the heavy hydrides, however, the changes in the angle α_s and the bond r_{3s} are insignificant, i.e., these quantities are stabilized beyond the critical region. (See Fig. 1). In the rigid bond models,[5,9] the valence angle is independent of J for $J>J_c$ and equals its value at the critical point. It should be noted that the contribution of the potential energy to the overall energy of the molecule in the S_z and S_{xz} states is small. For the H_2S, H_2Se, and H_2Te molecules at the critical point, the rotational energy forms more than 95% of the total energy. With increasing J, the contribution of the rotational energy decreases. For the same values of J as for the heavy hydrides, the potential energy fraction for the water molecule and the lighter molecules is greater. This circumstance, together with the fact that the equilibrium angle α_e increases as the mass of the central nucleus is reduced, leads to higher values of the critical momentum J_c. For the water molecule the fraction of potential energy increases to 20% beyond the critical region. The stabilization is disrupted as a result: the angle α_s continues to decrease (see Fig. 1) and r_{3s} increases, while r_{1s} begins to decrease for $J>50$.

4. PRECESSIONAL MOTION OF THE MOLECULE NEAR STATIONARY STATES

The shift in the stationary rotation regimes of the AB_2 molecule with increasing J can be traced by studying the stability of the stationary states using the linearized equations (14)–(16) for small deviations in the internal coordinates $Q_\nu=q_\nu-q_{\nu s}$ (vibrations) and in the projections of the angular momentum J_i-J_{is} (precession) from their stationary values. Let us begin with the stationary state S_y in which the vibrational motion is separated from the precession. Since $J_{xs}=J_{zs}=0$ holds in this state, while the momentum $p_{\nu s}$ is nonzero and given by Eq. (17), the precession equation has the form

$$\dot{J}_x+J^2(\mathring{\mu}_{xx}-\mathring{\mu}_{yy})(\mathring{\mu}_{zz}-\mathring{\mu}_{yy})J_x=0, \tag{29}$$

with the moments of inertia taken in the stationary state. Equation (29) coincides exactly with the precession equation for a solid asymmetric top.[27] The precession is stable, since its frequency

$$\Omega_y=J\sqrt{(\mathring{\mu}_{xx}-\mathring{\mu}_{yy})(\mathring{\mu}_{zz}-\mathring{\mu}_{yy})} \tag{30}$$

is real because $\mathring{\mu}_{xx}$ and $\mathring{\mu}_{zz}$ are always greater than $\mathring{\mu}_{yy}$.

The linearized equations of motion in the S_z state describe vibrational and precessional motion. Because of the symmetry of the molecule in this state, the equations break down into two independent subsystems. The coupled precession and asymmetric vibrations with coordinate $Q_a=(Q_1-Q_3)/\sqrt{2}$ obey the equations

$$\begin{aligned}&\ddot{Q}_a+\left[(b_{11}-b_{13})f_{aa}+2J^2u_{y1}\frac{\partial\mathring{\mu}_{xz}}{\partial q_1}\right]Q_a+\sqrt{2}J\\&\times\left[(b_{11}-b_{13})\frac{\partial\mathring{\mu}_{xz}}{\partial q_1}-(\mathring{\mu}_{zz}-\mathring{\mu}_{xx})u_{y1}\right]J_x=0,\\&\dot{J}_x+J^2\left[(\mathring{\mu}_{zz}-\mathring{\mu}_{yy})(\mathring{\mu}_{zz}-\mathring{\mu}_{xx})+2u_{y1}\frac{\partial\mathring{\mu}_{xz}}{\partial q_1}\right]J_x\\&\quad+\sqrt{2}J\left[u_{y1}f_{aa}-J^2(\mathring{\mu}_{zz}-\mathring{\mu}_{yy})\frac{\partial\mathring{\mu}_{xz}}{\partial q_1}\right]Q_a=0.\end{aligned} \tag{31}$$

We have introduced the force constant $f_{aa}=f_{11}-f_{13}$ for the asymmetric vibrations of the molecule using the matrix

$$f_{\nu\nu'}=\left(\frac{\partial^2V_{\text{eff}}}{\partial q_\nu\partial q_{\nu'}}\right)_s. \tag{32}$$

The two remaining vibrational modes, which are independent of the rotation, will be examined below.

The precessional motion can be separated from the asymmetric vibrations in the adiabatic approximation $\omega_3\gg\Omega_z$, which is valid up to the critical point J_c. In this approximation the precession frequency about the z axis equals

$$\Omega_z=J\sqrt{(\mathring{\mu}_{zz}-\mathring{\mu}_{yy})\left\{\mathring{\mu}_{zz}-\mathring{\mu}_{xx}+\frac{J^2}{f_{aa}}\left(\frac{\partial\mathring{\mu}_{xz}}{\partial r_a}\right)_s^2\right\}}, \tag{33}$$

where, according to Eqs. (3) and (10),

$$\mathring{\mu}_{zz}-\mathring{\mu}_{xx}=\frac{2(M+m)}{mMr_s^2\sin\alpha_s}\left(\frac{m}{M+m}-\cos\alpha_s\right). \tag{34}$$

For small J the last, nonadiabatic term in the curly brackets of Eq. (33) can be neglected. In this limit we obtain the precession frequency of a solid asymmetric top. It is real, since we are considering precession about the axis with the smallest moment of inertia and the angle α_e is greater than 90° for all the hydrides being considered. With increasing J, as we have seen, the stationary angle α_s decreases, $\mathring{\mu}_{zz}$ approaches $\mathring{\mu}_{xx}$, and the precession frequency Ω_z goes to zero when

$$\mathring{\mu}_{zz}-\mathring{\mu}_{xx}+\frac{J_c^2}{f_{aa}}\left(\frac{\partial\mathring{\mu}_{xz}}{\partial r_a}\right)_s^2=0. \tag{35}$$

Equations (35) and (18) determine the critical angular momentum J_c beyond which the stationary state S_z becomes unstable. The small nonadiabatic term in Eq. (35), which accounts for the deformability of the bonds, becomes important when the difference $\mathring{\mu}_{zz}-\mathring{\mu}_{xx}$ is small. Since it is positive, the critical angular momentum is greater, while the critical valence angle is less than the corresponding quantities in the rigid bond models. The critical angle α_c in the latter case is given by

$$\alpha_c=\cos^{-1}\left(\frac{m}{M+m}\right). \tag{36}$$

Note that the nonadiabatic term in Eq. (35) originates exclusively in the centrifugal inertia force. The Coriolis force, which changes the precession frequency by an amount of order $(\Omega_z/\omega_3)^2$, has no effect on the critical angular momentum J_c, which is explained by the planar configuration of the molecule.

The higher the asymmetric mode frequency ν_3 is, the closer J_c is to the value found[9] in the approximation of absolutely rigid bonds. Numerical calculations of the critical angular momentum for these hydrides using realistic potentials[13,15,16] are only slightly different from the previously determined values of J_c. We found $J_c=9.3$ for H_2Te, $J_c=12.5$ for H_2Se, and $J_c=18.9$ for H_2S. The corresponding values in the rigid bond models are 8.5, 11.4, and 16.9. It appears that the lighter the molecule, the greater the difference between these numbers. This difference is greatest for the water molecule. The potential of Ref. 19 gives $J_c=35.2$, which is much higher than the $J_c=26.5$ found in the approximation of rigid bonds.

For $J>J_c$ the stationary state S_z becomes a saddle point on the energy surface. It determines the maximum depth of the valley (a classically inaccessible region) separating the two symmetric maxima S_{xz} which develop as a result of the bifurcation. Near one of the maxima, the linearized equations of motion have a simple form in the coordinate system rotated about the y axis by an angle β_s (or $\pi-\beta_s$). The Hamiltonian and the equations of motion in this system are given by Eqs. (11) and (14)–(16) if the projection of the vector **J** and the elements of the matrix $\mathring{\mu}$ are related to the new primed axes. In this system, the total angular momentum vector of the state S_{xz} is directed along the z'. The linearized equations have the form

$$\begin{aligned}
&\ddot{Q}_\nu+\sum_{\nu'}\left[\sum_{\nu''} b_{\nu\nu''}f_{\nu''\nu'}+J^2u_{y\nu}\left(\frac{\partial\mathring{\mu}_{x'z'}}{\partial q_{\nu'}}\right)_s\right]Q_{\nu'}\\
&\quad+J\left[\sum_{\nu'} b_{\nu\nu'}\left(\frac{\partial\mathring{\mu}_{x'z'}}{\partial q_{\nu'}}\right)_s+(\mathring{\mu}_{x'x'}-\mathring{\mu}_{z'z'})u_{y\nu}\right]J_{x'}=0,\\
&\ddot{J}_{x'}+J^2\Bigg[(\mathring{\mu}_{z'z'}-\mathring{\mu}_{yy})(\mathring{\mu}_{z'z'}-\mathring{\mu}_{x'x'})\\
&\qquad+\sum_{\nu} u_{y\nu}\left(\frac{\partial\mathring{\mu}_{x'z'}}{\partial q_{\nu}}\right)_s\Bigg]J_{x'}+J\sum_{\nu}\left[\sum_{\nu'} u_{y\nu'}f_{\nu'\nu}\right.\\
&\qquad\left.-J^2(\mathring{\mu}_{z'z'}-\mathring{\mu}_{yy})\left(\frac{\partial\mathring{\mu}_{x'z'}}{\partial q_{\nu}}\right)_s\right]Q_\nu=0.
\end{aligned} \tag{37}$$

where the matrix elements $\mathring{\mu}_{i'j'}$ are given by Eqs. (22). This system of equations coincides in form with the linearized equations for the S_z with the sole difference that the three vibrational and precessional motions are not separated owing to the asymmetry of the molecule. Note that the force constant matrix $f_{\nu\nu'}$ differs from the matrix $g_{\nu\nu'}$ of Eq. (28). The second derivatives of the effective potential in the first case are calculated for a fixed angle β_s. These quantities are related by

$$\begin{aligned}
g_{\nu\nu'}=f_{\nu\nu'}+2[&(\mathring{\mu}_{z'z'}-\mathring{\mu}_{x'x'})^2\\
&+4\mathring{\mu}^2_{x'z'}]^{-1/2}\left(\frac{\partial\mathring{\mu}_{x'z'}}{\partial q_\nu}\right)_{\beta_s}\left(\frac{\partial\mathring{\mu}_{x'z'}}{\partial q_{\nu'}}\right)_{\beta_s},
\end{aligned} \tag{38}$$

where the subscript β_s indicates that the derivatives are taken for fixed values of this angle. Using the adiabatic approximation, we find the precession frequency for not too large J:

$$\Omega_{xz}=J\sqrt{(\mathring{\mu}_{z'z'}-\mathring{\mu}_{yy})\left[\mathring{\mu}_{z'z'}-\mathring{\mu}_{x'x'}+J^2\sum_{\nu\nu'}\left(\frac{\partial\mathring{\mu}_{x'z'}}{\partial q_\nu}\right)_s f^{-1}_{\nu\nu'}\left(\frac{\partial\mathring{\mu}_{x'z'}}{\partial q_{\nu'}}\right)_s\right]}. \tag{39}$$

It is easy to show that the frequency (39) goes to zero at the critical point J_c. Equation (39) is formally similar to Eq. (33) for the precession frequency in the S_z state, but the term in square brackets, which is proportional to J^2, is not small. It ensures that the frequency Ω_{xz} is real. At the critical point J_c this frequency goes to zero, since the expression in the square brackets of Eq. (39) transforms into the left hand side of Eq. (35).

The precessional–vibrational motion near the stationary state S_x obeys equations similar to Eq. (31) for the S_z state. Precession about this axis is unstable.

We now turn to the structure of the rotational multiplet levels. Equations (19) and (24) can be used to estimate with good accuracy the energies of the lower and upper levels in the multiplet for all J, including those in the $S_z\rightarrow S_{xz}$ transition region. The difference from experimental values or variational calculations for the H_2O, H_2S, H_2Se, and H_2Te molecules is less than 10%. The separatrix passing through the saddle point corresponding to the S_x state separates the region of precessional motion localized about the y or z axes and, therefore, determines the formation of K-doublets in the lower and upper parts of the multiplets.[3] Yet another separa-

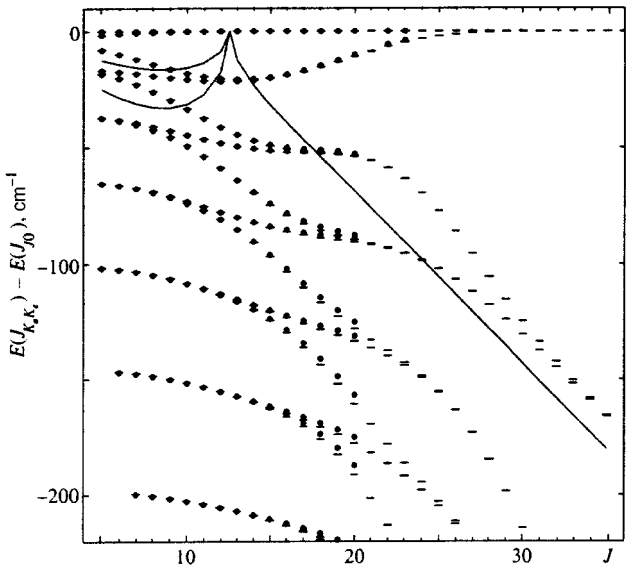

FIG. 2. Structure of the rotational levels of the upper parts of the J-multiplets of the ground vibrational state of the $H_2{}^{80}Se$ molecule. The multiplet levels are determined by the approximate quantum numbers for the projection of the angular momentum on the axes with the minimum (K_a) and maximum (K_c) moments of inertia. The energy of a level is taken relative to the energy of the upper level of the multiplet ($K_a=J$, $K_c=0$) and equals the experimental (points) or theoretical (dashes) value from Ref. 14. The smooth curves are a harmonic approximation with frequencies (33) and (39).

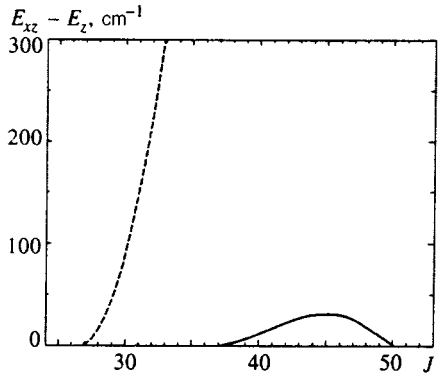

FIG. 3. The depth of the valley separating the two equivalent maxima of the S_{xz} state on the rotational energy surface of the water molecule calculated using Eqs. (19) and (24) (smooth curve) and in the approximation of absolutely rigid bonds (dashed curve).

trix of the S_z saddle arises as a result of the bifurcation. It separates the regions of precessional motion about the S_{xz} maxima and leads to clustering of the K-doublets. The depth of the valley between these maxima equals the energy difference between the stationary states S_{xz} and S_z. As J rises, this quantity increases in the H_2S, H_2Se, and H_2Te molecules and this shows up as a reduction in the splitting of the clustered levels. This behavior can be seen in Fig. 2, which shows the energy of the upper multiplet levels of the H_2Se molecule as a function of J. The energies given there have been calculated with the aid of the MORBID variational program[17] and the harmonic approximation of Eqs. (33) and (39) using the empirical potential from Ref. 13. The harmonic approximation clearly reproduces the qualitative behavior of the upper levels. It is not, however, applicable near the critical point and cannot describe level clustering.

The water molecule is a special case among the hydrides considered here. Calculations for this molecule with a new optimized potential from Ref. 19 show that the depth of the valley separating the S_{xz} maxima grows very slowly as the total angular momentum is increased. Figure 3 illustrates the qualitative difference between the models. While the valley rapidly becomes deeper with increasing J in the model of absolutely rigid bonds, in the calculations using Eqs. (20) and (21) its depth reaches a maximum at $J=45$ and then begins to decrease. The valley vanishes at $J=52$. This is a second critical point J_c' in the rotational spectrum where the two S_{xz} peaks merge into one S_z and for $J>J_c'$ the molecule is again rotating about the z axis. The two bifurcations are clearly visible in Fig. 1 from the characteristic breaks in the $\alpha_s(J)$ curve. The second critical point is too close to the first for a significant valley to form. Its maximum depth is comparable to the precession frequency. Thus, cluster levels similar to the levels in the heavy hydrides do not form in the water molecule. This provides a physical explanation for some numerical calculations[20] of the rotational spectrum of water. It is desirable to determine the molecular potential used there up to energies of order 10000 cm^{-1}, which corresponds to the potential energy at the point J_c'. Only then can we speak of the behavior of this molecule near the second critical point.

A type-C_{2v} bifurcation should also exist in the rotational spectra of the excited vibrational states, since the adiabatic approximation, and hence Eqs. (33) and (39), remain valid in this case. An analysis of experimental data[5,9] indicates that the upper levels of the rotational multiplets of the ν_2 vibrational state of the H_2O and H_2S molecules tend to cluster. Clusters have been found in rotational spectra of the ν_1/ν_3 vibrational states of the H_2Se (Refs. 13,14) H_2S, (Refs. 15) and H_2Te (Ref. 16) molecules using quantum mechanical variational calculations. Later, these clusters were observed experimentally in H_2Se, (Ref. 28) and H_2Te (Ref. 29).

5. VIBRATIONS OF A ROTATING MOLECULE

We now consider the change in the vibrational motion of a molecule during the transition at the critical point J_c. In the S_z stationary state ($J<J_c$) the adiabatic approximation gives the following equation of motion for the asymmetric mode ν_3:

$$\ddot{Q}_a+(b_{11}-b_{13})f_{aa}Q_a=0. \tag{40}$$

where, according to Eq. (13), $b_{13}\sim(m/M)b_{11}$. The symmetric ν_1 ($Q_{sm}=(Q_1+Q_3)/\sqrt{2}$) and bending ν_2 (Q_2) modes do not depend on the precession and obey the coupled equations

$$\begin{aligned}&\ddot{Q}_s+(b_{11}+b_{13})f_{ss}Q_{sm}+(b_{11}+b_{13})f_{s2}Q_2=0,\\&\ddot{Q}_2+(b_{22}f_{22}+\sqrt{2}b_{12}f_{s2})Q_2+(b_{22}f_{s2}+\sqrt{2}b_{12}f_{ss})Q_{sm}=0.\end{aligned} \tag{41}$$

where $f_{ss}=f_{11}+f_{13}$ and $f_{s2}=\sqrt{2}f_{12}$, with $f_{11}=f_{33}$ and $f_{23}=f_{12}$ owing to the symmetry of the molecule in the S_z state. (See the definition of the force constants (32).) Clearly,

TABLE II. Normalized amplitudes of the internal coordinates and components of the total angular momentum of the four vibrational–precessional modes of the H_2Se molecule in the stationary S_z state for $J=10$.

Frequency, cm^{-1}	Normalized amplitudes			
	r_1-r_{1s}, Å	$\alpha-\alpha_s$, rad	r_3-r_{3s}, Å	J_x/J
$\omega_1=2426$	1*	−0.032	1.000	0
$\omega_2=1082$	−0.014	1*	−0.014	0
$\omega_3=2437$	−1.000	0	1*	0.004
$\Omega_z=16$	0.004	−0.004	0	1*

Note. *The normalization condition is $Q_n=1$.

TABLE III. Normalized amplitudes of the internal coordinates and components of the total angular momentum of the four vibrational–precessional modes of the H_2Se molecule in the stationary S_{xz} state for $J=40$ (the molecule rotates uniformly about an axis that forms an angle $\beta_s=42°$ with the z axis).

Frequency cm^{-1}	Normalized amplitudes			
	r_1-r_{1s}, Å	$\alpha-\alpha_s$, rad	r_3-r_{3s}, Å	$J_{x'}/J$
$\omega_1=2096$	1*	0.030	0.015	0.004
$\omega_2=1272$	−0.022	1*	−0.009	0.093
$\omega_3=2438$	−0.015	0.003	1*	−0.002
$\Omega_{xz}=212$	0	0.429	−0.009	1*

Note. *The normalization condition is $Q_n=1$.

the coupling takes place through the mixed derivatives of V_{eff} and the nondiagonal element b_{12}. The parameters

$$\frac{b_{11}f_{s2}}{b_{11}f_{ss}-b_{22}f_{22}}, \quad \frac{b_{12}f_{ss}}{b_{11}f_{ss}-b_{22}f_{22}}. \tag{42}$$

which determine the mode coupling, are small owing to the condition (27) and the inequality $m/M\ll 1$. Thus, for the hydrides the mode interaction is weaker and this allows us to classify the molecular vibrations in the S_z state according to the standard scheme:[22] the frequency ω_1 corresponds to symmetric valence vibrations ν_1, ω_3 to the asymmetric ν_3 mode, and ω_2 to the bending ν_2 mode. Unlike a nonrotating molecule, the centrifugal force of inertia changes the frequency of all the vibrations. This is illustrated in Table II, which lists the normalized coordinate amplitudes Q_1, Q_2, Q_3, and $Q_4=J_x/J$ for all four precessional–vibrational modes of the H_2Se molecule. These data were obtained by numerically solving the linearized equations for $J=10$. It is clear from the table that the interaction of the vibrational modes among themselves and with the precessional motion is indeed small.

The character of the vibrational motion changes radically after the critical point J_c. In the S_{xz} state the molecule becomes asymmetric, which leads to mixing of all three vibrational modes among themselves and with precession. For J that is not too large, the adiabatic approximation makes it possible to separate the vibrational motion, for which, according to Eq. (37), the equations have the form

$$\ddot{Q}_\nu+\sum_{\nu'\nu''} b_{\nu\nu'}f_{\nu'\nu''}Q_{\nu''}=0. \tag{43}$$

They describe the coupled local vibrations Q_1, Q_2, and Q_3. And again, coupling takes place through the mixed derivatives and nondiagonal elements of the matrix **b**. Since the inequality

$$\sum_{\nu''} \frac{b_{\nu\nu''}f_{\nu''\nu'}}{|b_{\nu\nu}f_{\nu\nu}-b_{\nu'\nu'}f_{\nu'\nu'}|}\ll 1, \quad \nu\neq\nu', \tag{44}$$

is satisfied for all the hydrides, the three local modes are quasi-independent vibrations. This effect is illustrated in Table III, which shows the normalized amplitudes of the vibrational–precessional motion of the H_2Se molecule given by Eq. (37) for $J=40$. The precession in the total angular momentum corresponds to the dimensionless variable $Q_4=J_{x'}/J$. It is clear that the precessional motion is mixed most strongly with bending vibrations.

Therefore, beyond the critical region the standard picture of the normal vibrations of symmetric triatomic molecules is not applicable. We note that the same result has been obtained in numerical calculations using the MORBID program.[14,15] Because of the asymmetry of the molecule, the elastic coupling constants of the central nucleus with the hydrogen nuclei become different. The difference becomes greater as J and the mass of the molecule increase, and this leads to a characteristic pattern in the vibrations for the local modes.[23] Usually the local modes arise as a result of the strong anharmonicity of the highly excited valence vibrations. In our case, the transition from normal to local vibrations takes place as a result of rotational excitation which disrupts the symmetry of the molecule owing to a bifurcation.

In the stationary S_y state, the vibrational motion independent of precession is described by the equation

$$\ddot{Q}_\nu+\sum_{\nu'\nu''} b_{\nu\nu'}(Jh_{\nu'\nu''}\dot{Q}_{\nu''}+f_{\nu'\nu''}Q_{\nu''})=0. \tag{45}$$

The Coriolis force leads to an additional interaction of the vibrational modes which corresponds in Eq. (45) to the term with the first derivative and the antisymmetric matrix

$$h_{\nu\nu'}=\left[\frac{\partial(\mathring{\mu}_{yy}G_{y\nu})}{\partial q_{\nu'}}-\frac{\partial(\mathring{\mu}_{yy}G_{y\nu'})}{\partial q_\nu}\right]_s. \tag{46}$$

Since the molecule has a symmetric configuration in the S_y state, only one element of this matrix, $h_{12}\simeq -1/2r_s$, is nonzero. If in Eq. (46) we transform to the variables Q_{sm} and Q_a for the valence vibrations, use the smallness of the parameters (42), and neglect the nondiagonal terms b_{12} and b_{13} compared to the diagonal terms b_{11} and b_{22}, which are a factor of M/m greater than the former, then the symmetric valence vibrations are separated, while the antisymmetric and bending modes obey the coupled system of equations

$$\begin{aligned}&\ddot{Q}_a+b_{11}(\sqrt{2}Jh_{12}\dot{Q}_2+f_{aa}Q_a)=0,\\ &\ddot{Q}_2+b_{22}(-\sqrt{2}Jh_{12}\dot{Q}_a+f_{22}Q_2)=0.\end{aligned} \tag{47}$$

It is easy to see that the coupling parameter in these vibrations is of order $\omega/(\omega_3-\omega_2)$, where ω is the angular rotation frequency of the molecule. Since the difference in the frequencies of the two normal modes is $\omega_3-\omega_2\sim 1000\ cm^{-1}$ for the heavy hydrides, the coupling

TABLE IV. Normalized vibration amplitudes of the H_2Se molecule in the stationary S_y state for $J=40$.

Frequency, cm^{-1}	Normalized amplitudes		
	r_1-r_{1s}, Å	$\alpha-\alpha_s$, rad	r_3-r_{3s}, Å
$\omega_1=2346$	1*	0.031	1.000
$\omega_2=1030$	−0.014	1*	−0.014
$\omega_3=2278$	−0.992	0.001	1*

Note. *The normalization condition is $Q_n=1$.

parameter is small if $J<100$. For these angular momenta the Coriolis force does not lead to significant distortion of the fundamental modes. This is illustrated by Table IV, which lists the normalized vibration amplitudes obtained by numerical solution of the exact equations (45). The table does not show the tiny phase shift in the coordinates of the normal vibrations owing to the Coriolis interaction.

The authors thank the Russian Fund for Fundamental Research for partial support of this work through grants Nos. 96-02-16115 and 97-02-16593. One of the authors (I.N.K.) thanks PECO and CIES for providing a stipend.

[1)]This quantity is measured in units of $\hbar$ in the following.

[1] A. J. Dorney and J. K. G. Watson, J. Mol. Spectrosc. **42**, 135 (1972).
[2] W. G. Harter and C. W. Patterson, J. Chem. Phys. **80**, 4241 (1984).
[3] W. G. Harter, Comput. Phys. Rep. **8**, 319 (1988).
[4] D. A. Sadovskii, B. I. Zhilinskii, J.-P. Champion, and G. Pierre, J. Chem. Phys. **92**, 1523 (1990).
[5] B. I. Zhilinskiĭ and I. M. Pavlichenkov, Opt. i Spektr. **64**, 688 (1988).
[6] J. T. Hougen, P. R. Bunker, and J. W. C. Johns, J. Mol. Spectrosc. **34**, 136 (1970).
[7] I. M. Pavlichenkov, Phys. Rep. **226**, 175 (1993).
[8] J. Makarewicz and J. Pyka, Mol. Phys. **68**, 107 (1989); J. Makarewicz, Mol. Phys. **69**, 903 (1990); J. Pyka, Mol. Phys. **70**, 547 (1990).
[9] I. M. Pavlichenkov, in *Physics of the Atomic Nucleus (Material from the XXIV Winter School at the Leningrad Inst. of Nuclear Physics, Leningrad (1989)* [in Russian], Leningrad Inst. of Nuclear Physics, Leningrad (1989), p. 69.
[10] I. N. Kozin, S. P. Belov, O. I. Polyansky, and M. Yu. Tretyakov, J. Mol. Spectrosc. **152**, 13 (1992).
[11] I. N. Kozin, S. Klee, P. Jensen, O. I. Polyansky, and I. M. Pavlichenkov, J. Mol. Spectrosc. **158**, 409 (1993).
[12] I. N. Kozin, P. Jensen, O. Polanz, S. Klee, L. Poteau, and J. Demaison, J. Mol. Spectrosc. **180**, 402 (1996).
[13] P. Jensen and I. N. Kozin, J. Mol. Spectrosc. **160**, 139 (1993).
[14] I. N. Kozin and P. Jensen, J. Mol. Spectrosc. **161**, 186 (1993).
[15] I. N. Kozin and P. Jensen, J. Mol. Spectrosc. **163**, 483 (1994).
[16] P. Jensen, Yan Li, G. Hirsch, R. J. Buenker, T. H. Lee, and I. N. Kozin, Chem. Phys. **180**, 179 (1995).
[17] P. Jensen, J. Mol. Spectrosc. **128**, 478 (1988); J. Chem. Soc. Faraday Trans. 2, **84**, 1315 (1988).
[18] P. Jensen and I. N. Kozin, unpublished results.
[19] P. Jensen, J. Mol. Spectrosc. **133**, 438 (1989); P. Jensen, S. Tashkun, and V. G. Tyuterev, J. Mol. Spectrosc. **168**, 271 (1994).
[20] O. L. Polyansky, P. Jensen, and J. Tennyson, J. Chem. Phys. **101**, 7651 (1994).
[21] I. N. Kozin and I. M. Pavlichenkov, J. Chem. Phys. **104**, 4105 (1996).
[22] E. Wilson, J. Decius, and P. Cross, *Molecular Vibrations: the Theory of Infrared and Raman Vibrational Spectra*, McGraw-Hill, N. Y. (1955).
[23] M. S. Child and I. Halonen, Adv. Chem. Phys. **57**, 1 (1984).
[24] B. T. Sutcliffe and J. Tennyson, Mol. Phys. **58**, 1053 (1986); Int. J. Quantum Chem. **39**, 183 (1991).
[25] P. R. Bunker *Molecular Symmetry and Spectroscopy*, Academic Press, London (1979)
[26] P. Jensen and P. R. Bunker, J. Mol. Spectrosc. **164**, 315 (1994).
[27] L. D. Landau and E. M. Lifshitz, *Mechanics* 3rd ed., Pergamon, Oxford (1976).
[28] J.-M. Fland, C. Camy-Peyret, H. Bürger, P. Jensen, and I. N. Kozin, J. Mol. Spectrosc. **172**, 194 (1995).
[29] J.-M. Flaud, M. Betrencourt, Ph. Arcas, H. Bürger, O. Polanz, and W. J. Lafferty, J. Mol. Spectrosc. **182**, 396 (1997).

Translated by D. H. McNeill